Received November 25, 2017, accepted January 1, 2018, date of publication January 5, 2018, date of current version February 28, 2018.

Digital Object Identifier 10.1109/ACCESS.2018.2789914

Optimal Spectrum Sensing Interval in MISO Cognitive Small Cell Networks

BOYANG LIU[1], YINGYU BAI[1], GUANGYUE LU[1], JIN WANG[1], AND HAIYAN HUANG[2]

[1]School of Communications and Information Engineering, Xi'an University of Posts and Telecommunications, Xi'an 710121, China

[2]School of Electronic and Information Engineering, Lanzhou Jiaotong University, Lanzhou 730070, China

Corresponding authors: Boyang Liu (boyangliulby@163.com) and Guangyue Lu (tonylugy@163.com)

This work was supported in part by the National Natural Science Foundation of China under Grant 61701399 and Grant 61501371, in part by the Natural Science Foundation of Xizang under Grant 2016ZR-MZ-01, and in part by the Research Program of Education Bureau of Shaanxi Province under Grant 17JK0699.

ABSTRACT This paper considers a cognitive small cell network, where one cognitive base station (CBS) transmits information to the cognitive user and energy to the energy harvesting receivers (EHRs). The Markov channel model is exploited to characterize the state change of the macrocell base station. The spectrum sensing time, the spectrum sensing interval, and the beamforming matrixes of the CBS are jointly optimized to achieve three goals: the maximization of the CBS throughput, the minimization of the energy cost of the CBS, and the minimization of the interferences to the macrocell users (MUEs). These objectives are optimized subject to the interference constraints of the MUEs, the secrecy rate constraint, the transmit power constraint of the CBS, and the energy harvesting constraints of the EHRs. The formulated problems are challenging non-convex and difficult to solve. A 1-D line search method and semidefinite relaxation-based algorithm is proposed to solve these problems. It is proved that the optimal solution can be obtained under some conditions. If the conditions are not satisfied, Gaussian randomization procedure is used to obtain the suboptimal solutions. Simulation results verify our theoretical findings and demonstrate the effectiveness of the proposed resource allocation scheme.

INDEX TERMS Cognitive small cell, non-linear energy harvesting, Markov chain, spectrum sensing interval, beamforming.

I. INTRODUCTION

The explosive increase of the wireless service requirements are expected to be satisfied in the fifth generation (5G) systems, which have many advantages over the current wireless communication systems such as lower latency, massive connectivity, etc. [1]. One of the key technologies of 5G systems is small cell, which can effectively improve the spectrum efficiency by narrowing the cell coverage at the cost of excessive inter-cell interferences and higher hardware costs [2]–[4].

Another promising technology to improve the spectrum efficiency is cognitive radio (CR). In CR networks, the secondary users (SUs) execute spectrum sensing to obtain the status of the primary users (PUs) and adjust the transmit power to access the spectrum bands of the PUs, while satisfying the PUs interference limitations [5], [6]. By adopting CR technology, the spectrum efficiency can be improved without changing much hardware architectures of the current wireless communication systems. Therefore, CR can play an important role in 5G small cells to further enhance the spectrum efficiency, which can make a tradeoff among the spectrum efficiency, inter-cell interferences and the hardware cost.

A. RELATED WORK AND MOTIVATION

Spectrum sensing, interference mitigation and power control are three main tasks of CR small cells [3], [7]–[9]. There exists lots of spectrum sensing algorithms such as matched filter detection [10], [11], energy detection [12], [13], cyclostationary based detection [14], [15], and the covariance based detection [16], [17]. Each of these algorithms has its own advantages and disadvantages [18]. Interference mitigation is a primary challenge in deploying the small cell, which can be realized by power control. An extensive interference analyses were provided in [19], which included interferences on macrocell users (MUEs) from small cell users, inter-cell interference among small cells users, interferences from other users within one small cell, etc. Based on the interference measurements, a stochastic dual control method was proposed to adapt the spectrum sensing process to mitigate the interference in small cells. The transmit power and the spectrum sensing time were jointly optimized to maximize the energy efficiency in a cognitive small cell, where the cross-tier interference and transmit power constraint were considered [2], [20]. Cheng *et al.* [21] derived the bounds of the maximum intensity of simultaneously transmitting small cells that satisfied a given per-tier outage constraint. A joint optimization of decision threshold and transmit power scheme was proposed to maximize the opportunistic throughput, under the MUEs interference constraints [22]. Considered the cross-tier interference limitation, minimum outage probability requirement and imperfect CSI, the joint sub-channel and power allocation problem in cognitive small cell was solved in [23] by using cooperative Nash bargaining game. Small cell users can cooperate with the MUEs to achieve some performance gain. Two cooperation modes between small cell users and MUEs were proposed in [24], namely, cooperative relay mode and interference control mode. In order to maximize the throughput of the small cell users, the small cell users chosen to be a relay node to enhance the MUE's transmit rate or to stop its own transmission to reduce the interferences caused to the MUEs [24]. A dynamic selection scheme of overlay/underlay modes was proposed in [25], which considered the small cell users throughput and the energy consumption. Xie *et al.* [26] considered a different wireless network architecture that the both the MUE and the small cell users had cognitive capability. And an energy-efficient resource allocation algorithm based on Stackelberg game was proposed in heterogeneous CR networks.

It can be noted that all the aforementioned works were based on the traditional slot structure, i.e., a slot consists of a spectrum sensing subslot and a transmission subslot. The SUs execute spectrum sensing at the beginning of each slot, i.e, the spectrum sensing interval is 1. The spectrum sensing interval is defined as the number of slots during which the channel state of the PU is considered unchanged and no further spectrum sensing is required [27]. In some practical scenarios, the access pattern of the PU can be characterized by a statistical model, the future status of the PUs can be predicted to some extent [27]–[33]. Therefore, the spectrum sensing interval does not necessarily to be set to 1. Setting the spectrum sensing interval bigger than 1 has some advantages. Firstly, adopting larger spectrum sensing interval may save the spectrum sensing energy, which can be used for the data transmission of the SUs. Secondly, adopting lager spectrum sensing interval will save the time for spectrum sensing, which also can be used for data transmission to enhance the throughput of SUs. Thirdly, setting the spectrum sensing interval to 1, the spectrum sensing scenario that the PU has statistical characteristics become the traditional spectrum sensing scenario. However, it is hard to accurately predict the future status of the PU even though the access pattern of the PU has statistical property. The SU will transmit multiple consecutive slots after executing the spectrum sensing once, which may collide with the PU's transmission. Therefore, the spectrum sensing interval and the transmit power must be carefully designed, which has already been studied in [27], [32] and [33]. The spectrum sensing interval was optimized at different spectrum sensing results in [27], but the spectrum sensing result was assumed to be perfect. Imperfect spectrum sensing was considered to jointly optimize the spectrum sensing interval, the spectrum sensing energy and the transmit power to maximize the degree of CR network satisfaction [32], [33]. However, all of these works did not take the communication security between the SUs into consideration. Moreover, these works only considered the single-input single-output (SISO) systems, which can not be applied into 5G systems.

B. MAIN CONTRIBUTIONS

In this paper, we focus on the downlink of a multiple-input single-output (MISO) CR small cell. The macrocell base station (MBS) and MUEs are PUs and the cognitive base station (CBS) and the cognitive users (CUEs) are SUs. It is assumed that the access pattern of the MBS has Markov property. The spectrum sensing interval, spectrum sensing time and the beamforming matrixes of the CBS are jointly optimized to achieve three goals. The first one is to maximize the throughput of the CBS, while the interference constraints of the MUEs, the CBS transmit power constraint, the energy harvesting constraints of energy harvesting receivers (EHRs) and the secrecy rate constraint are considered. The second one is to minimize the energy cost of the CBS, while the throughput of the CBS constraint, MUEs interference constraints, the CBS transmit power constraint, the energy harvesting constraints of EHRs and the secrecy rate constraint are considered. The third one is to minimize the interference to the MUEs, while the throughput of the CBS constraint, the CBS transmit power constraint, the energy harvesting constraints of EHRs and the secrecy rate constraint are considered. All of these three optimization problems are non-covex and rank-constrained optimization problems. Three conditions that the optimization problems have rank-one solutions are derived. We now summarize the main contributions of this paper as follows:

- The spectrum sensing interval optimization problem in the MISO scenario is studied. Although the spectrum sensing interval optimization problem has been studied in [27], [32] and [33], but the optimization problems in these works were studied in the SISO scenario, which is limited in 5G systems. We extend this problem to a more general multiple-input single-output (MISO) scenario.
- Three optimization objects are investigated from the viewpoints of the CBS and the MUEs, respectively. The corresponding three optimization objects are given as follows: the maximization of throughput of the CBS, the minimization of the energy cost of the CBS, the minimization of the interferences to the MUEs. Each of these optimization objects is achieved by jointly designing spectrum sensing time, transmit beamforming matrixes and spectrum sensing interval under the constraints

mentioned above. All of these problems are non-convex and solved by using semidefinite relaxation (SDR), one dimensional line search method and the software CVX. For each optimization problem, the conditions under which the problem has rank-one solutions are given.
- Extensive simulation studies have been conducted and the results indicate that when the state changes of MBS has Markov property, our proposed algorithms have higher throughput and greater dynamic range than the traditional spectrum sensing scheme.

The rest of this paper is organized as follows. Section II presents the system model. In Section III, we formulate the spectrum sensing time, spectrum sensing interval and beamforming matrixes joint optimization problems and solve them by using two dimensional line search method, SDR and CVX. The performance of the proposed algorithms are evaluated by simulation results in Section IV. Finally, Section V concludes this paper.

Notations: Matrices and vectors are denoted by boldface capital letters and boldface lower case letters, respectively. $\mathbf{I}$ denotes the identity matrix with size N_t, which is the number of the CBS transmit antennas. $(\cdot)^H$, $\mathrm{Tr}(\cdot)$ and $\mathrm{Rank}(\cdot)$ denote the Hermitian (conjugate) transpose, trace, and rank of a matrix, respectively. $\mathbf{C}^{M\times N}$ denotes a M-by-N dimensional complex matrix set. $\mathbf{X} \succeq \mathbf{0}\,(\mathbf{X} \succ \mathbf{0})$ represents that $\mathbf{X}$ is a Hermitian positive semidefinite matrix. $\mathbb{X}^N$ represents a N-by-N dimensional Hermitian matrix set.

II. SYSTEM MODEL

A. CR NETWORK MODEL

Consider a cognitive small cell laid within a macrocell network as shown in Fig. 1, where one CUE link, J MUE links, K EHR links share the same spectrum. The CBS is equipped with N_t antennas. MUEs, CUE, EHRs are equipped with single antenna. All users are assumed to operate in a synchronized time slot structure with time slot length T. The CBS transmits information to the CUE and transfer energy to the K EHRs, respectively. The MBS transmits information to J MUEs, which are assumed to be friendly and will not eavesdrop the information sent by the CBS. We use H_0 and H_1 denote the hypotheses that the MBS is busy and idle, respectively. The received signals transmitted by the CBS at the CUE, the kth EHR and the jth MUE can be given as

$$y_{IR} = \mathbf{h}^H \mathbf{w}_i s + n_{IR}, \quad i = 0, 1 \tag{1}$$

$$y_{ER_k} = \mathbf{g}_k^H \mathbf{w}_i s + n_{ER_k}, \quad i = 0, 1, \ k \in \kappa \tag{2}$$

$$y_{MUE_j} = \mathbf{u}_j^H \mathbf{w}_i s + n_{MUE_j}, \quad i = 0, 1, \ j \in \ell \tag{3}$$

where $\kappa = \{1, 2, \cdots, K\}$, $\ell = \{1, 2, \cdots, J\}$. $\mathbf{w}_i \in C^{N_t \times N_t}$, $i = 0, 1$ is the beamforming vector when the spectrum sensing result is H_i. $s \in \mathbf{C}^{1\times 1}$ denotes the transmit data symbol of the CBS which is assumed that $E\left(|s|^2\right) = 1$. n_{IR}, n_{ER_k} and n_{MUE_j} are the additive white Gaussian noises (AWGN) with mean 0 and variance N_0. $\mathbf{h} \in \mathbf{C}^{N_t\times 1}$, $\mathbf{g}_k \in \mathbf{C}^{N_t\times 1}$ and $\mathbf{u}_j \in \mathbf{C}^{N_t\times 1}$ denote the channel vectors between the CBS and the CUE, the kth EHR and the jth MUE, respectively. It is assumed that all the channel vectors do not change within the channel coherence time, which is assumed to be an integral multiple of T for convenience.

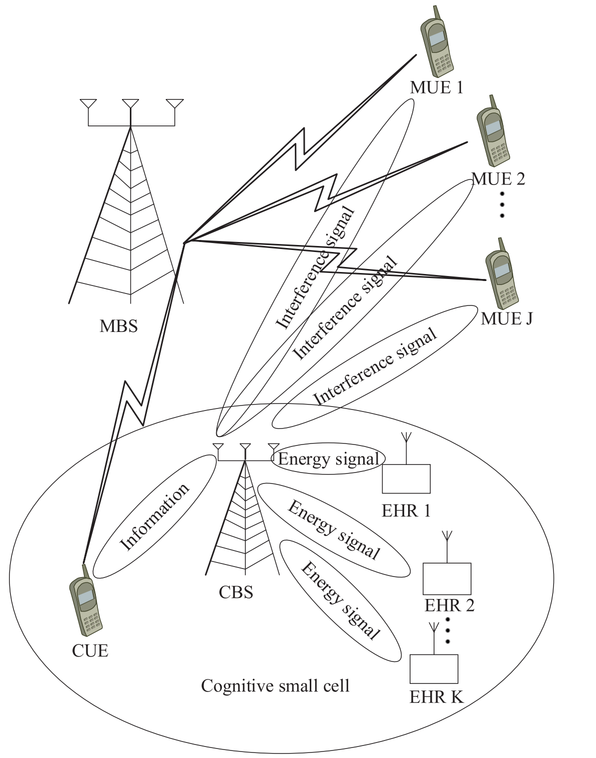

FIGURE 1. System model.

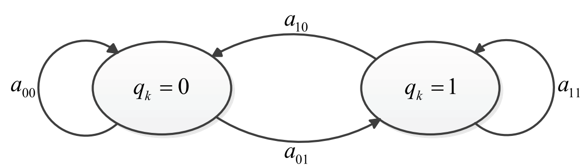

FIGURE 2. Markov channel model.

B. MBS ACTIVITY MODEL

We model the MBS states as a two-states on-off Markov chain as shown in Fig. 2, which has been widely used in CR networks [27]–[33]. The transition matrix is denoted by

$$\mathbf{A} = \begin{bmatrix} a_{00} & a_{01} \\ a_{10} & a_{11} \end{bmatrix} \tag{4}$$

where $a_{ij} = \Pr\left\{q_{t+1} = H_j | q_t = H_i\right\}, i, j = 0, 1$, q_t is the state of the MBS at slot t. The initial distribution of the states is assumed to be in a steady state and defined as

$$\boldsymbol{\pi} = \left[\frac{a_{10}}{a_{01} + a_{10}} \frac{a_{01}}{a_{01} + a_{10}}\right]. \tag{5}$$

C. NON-LINEAR ENERGY HARVESTING MODEL

One way to prolong the operation time of the cell users is to using EH technology [34], [35]. The received radio frequency (RF) power at the kth EHR is given as

$$P_{EHR_k} = \mathrm{Tr}\left(\mathbf{W}_i \mathbf{G}_k\right), \quad i = 0, 1, \ k \in \kappa \tag{6}$$

where $\mathbf{G}_k = \mathbf{g}_k\mathbf{g}_k^H$. $\mathbf{W}_i = \mathbf{w}_i\mathbf{w}_i^H, i = 0, 1$ denote the beamforming matrix of the CBS when the sensing result of the status of the MBS is $H_i, i = 0, 1$.

Unlike the traditional linear energy harvesting model, we adopt a non-linear energy harvesting model, which is proved to accurately illustrate the process of energy harvesting in practice [36]–[38]. According to the energy harvesting model, the harvested power at the kth EHR is given by [36]

$$\Phi_{EHR_k} = \frac{\Psi_{EHR_k} - M_k Z_k}{1 - Z_k} \tag{7}$$

where

$$\Psi_{EHR_k} = \frac{M_k}{1 + \exp\left(-a_k\left(P_{ER_k} - b_k\right)\right)} \tag{8}$$

$$Z_k = \frac{1}{1 + \exp\left(a_k b_k\right)} \tag{9}$$

where M_k is a constant denoting the maximum harvested power at the kth EHR when the energy harvesting circuit is saturated. Z_k denotes the maximum harvested power of the kth EHR, a_k and b_k are constants that capture the joint effects of resistance, capacitance, and circuit sensitivity [36].

III. PROBLEM FORMULATION

The goals of this section are to maximize the throughput of the CBS, minimize the energy cost of the CBS and minimize the interference to the MUEs, while satisfying the corresponding constraints.

Let random variable X_0 denote the number of the idle slots during Ω consecutive slots. When the current true channel state is busy, the mean of X_0 is given as [32], [33]

$$E(X_0)_{busy} = \begin{cases} \sum_{k=1}^{\Omega}\sum_{m=0}^{\Omega-1} \Pr\left(X_0 = k\right)k, & \Omega > 1 \\ 0, & \Omega = 1 \end{cases} \tag{10}$$

where m is the number of state changes during Ω consecutive slots. $\Pr\left(X_0 = k\right)$ is given as

$$\Pr\left(X_0 = k\right) = \begin{cases} \Pr_1\left(X_0 = k\right), & \text{if m is odd}, \\ & \frac{m+1}{2} \le k \le \Omega - \frac{m+1}{2} \\ \Pr_2\left(X_0 = k\right), & \text{if m is even}, \\ & \frac{m}{2} \le k \le \Omega - \frac{m+2}{2}, \\ & m > 0 \\ 0, & \text{otherwise} \end{cases} \tag{11}$$

where $\Pr_1\left(X_0 = k\right) = \binom{k-1}{\frac{m-1}{2}}\binom{\Omega-k-1}{\frac{m-1}{2}}$ $a_{11}^{\Omega-k}a_{00}^{k}\left(\frac{a_{10}a_{01}}{a_{11}a_{00}}\right)^{\frac{m+1}{2}}a_{01}^{-1}$, $\Pr_2\left(X_0 = k\right) = \binom{k-1}{\frac{m-2}{2}}\binom{\Omega-k-1}{\frac{m}{2}}a_{11}^{\Omega-k}$ $a_{00}^{k}\left(\frac{a_{10}a_{01}}{a_{11}a_{00}}\right)^{\frac{m}{2}}a_{11}^{-1}$ [32], [33]. When the current true channel state is idle, the expectation of X_0 is given as [32], [33]

$$E(X_0)_{idle} = \begin{cases} \sum_{k=1}^{\Omega}\sum_{m=0}^{\Omega-1} \Pr\left(X_0 = k\right)k, & \Omega > 1 \\ 1, & \Omega = 1 \end{cases} \tag{12}$$

where

$$\Pr\left(X_0 = k\right) = \begin{cases} \Pr_3\left(X_0 = k\right), & \text{if m is odd}, \\ & \frac{m+1}{2} \le k \le \Omega - \frac{m+1}{2} \\ \Pr_4\left(X_0 = k\right), & \text{if m is even}, \\ & \frac{m+2}{2} \le k \le \Omega - \frac{m}{2}, \\ & m > 0 \\ a_{00}^{\Omega-1}, & \text{if m} = 0 \\ 0, & \text{otherwise} \end{cases} \tag{13}$$

where $\Pr_3\left(X_0 = k\right) = \binom{k-1}{\frac{m-1}{2}}\binom{N_t-k-1}{\frac{m-1}{2}}a_{00}^{k}$ $a_{11}^{\Omega-k}\left(\frac{a_{10}a_{01}}{a_{11}a_{00}}\right)^{\frac{m+1}{2}}a_{10}^{-1}$ and $\Pr_4\left(X_0 = k\right) = \binom{k-1}{\frac{m}{2}}\binom{\Omega-k-1}{\frac{m-2}{2}}$ $a_{00}^{k}a_{11}^{\Omega-k}\left(\frac{a_{10}a_{01}}{a_{11}a_{00}}\right)^{\frac{m}{2}}a_{00}^{-1}$ [32].

We have assumed that the channel coherence time is an integer multiple of the length of a slot, which is denoted as d. Let $\Omega_i, i = 0, 1$, denote a variable that the probability of the state i lasting for more than Ω_i slots is less than 0.99, which is given in [32]. Then, the maximum spectrum sensing interval is defined as

$$\Omega_{max} = \min\left\{d, \max\left(\Omega_0, \Omega_1\right)\right\}. \tag{14}$$

Without loss of generality, we use energy detector to perform spectrum sensing in our work. A constant detection probability $\overline{P}_d$ is specified to protect the MUEs. Then, the false alarm probability P_f is given by [39]

$$P_f = Q\left(\sqrt{2\gamma + 1}Q^{-1}\left(\overline{P}_d\right) + \sqrt{\tau f_s}\gamma\right) \tag{15}$$

where γ is the received signal-to-noise ratio (SNR) of the MBS signal at the CBS. τ is the sensing time and f_s is the sampling frequency of the CBS. The energy consumed by energy detector is roughly linear in the number of samples, similar to [33] and [40], we assume $\tau = c_s e_s$, where c_s is a constant. Therefore, P_f is a function of e_s for given $\overline{P}_d$, which can be denoted as $P_f\left(e_s\right)$. Let H_{true} denote the true status of the MBS, $\widehat{H}$ denote the sensing result of the MBS. Then, there are four cases of $\left(H_{true}, \widehat{H}\right)$. The CBS throughput and the energy cost of the CBS during Ω consecutive slots (namely, the spectrum sensing interval is Ω) corresponding to case $\left(H_{true}, \widehat{H}_0\right) = \left(i, j\right), i, j = 0, 1$ are denoted as R_{ij} and e_{ij}, respectively. Let $\mathbf{H} = \mathbf{h}\mathbf{h}^H$ and q denotes the received MBS signal strength at the CUE. When the spectrum sensing interval is Ω, the CBS senses the status of the MBS at the beginning of Ω consecutive slots and transmits data at $\Omega - \frac{\tau}{T}$ slots. Then, the throughput and energy cost of the CBS for the four different cases as

$$R_{00} = \frac{1}{\Omega T}\left\{\left[E(X_0)_{idle}T - \tau\right]\log_2\left(1+\frac{\mathrm{Tr}\left(\mathbf{W}_0\mathbf{H}\right)}{\sigma^2}\right)\right. \left. + \left(\Omega - E(X_0)_{idle}\right)T\log_2\left(1+\frac{\mathrm{Tr}\left(\mathbf{W}_0\mathbf{H}\right)}{q+\sigma^2}\right)\right\} \quad (16)$$

$$e_{00} = e_s + \mathrm{Tr}\left(\mathbf{W}_0\right)\left(\Omega T - \tau\right) \quad (17)$$

$$R_{01} = \frac{1}{\Omega T}\left\{\left[E(X_0)_{idle}T - \tau\right]\log_2\left(1+\frac{\mathrm{Tr}\left(\mathbf{W}_1\mathbf{H}\right)}{\sigma^2}\right)\right. \left. + \left(\Omega - E(X_0)_{idle}\right)T\log_2\left(1+\frac{\mathrm{Tr}\left(\mathbf{W}_1\mathbf{H}\right)}{q+\sigma^2}\right)\right\} \quad (18)$$

$$e_{01} = e_s + \mathrm{Tr}\left(\mathbf{W}_1\right)\left(\Omega T - \tau\right) \quad (19)$$

$$R_{10} = \frac{1}{\Omega T}\left\{E(X_0)_{busy}T\log_2\left(1+\frac{\mathrm{Tr}\left(\mathbf{W}_0\mathbf{H}\right)}{\sigma^2}\right)\right. \left. + \left(\Omega - E(X_0)_{busy} - \frac{\tau}{T}\right)T\log_2\left(1+\frac{\mathrm{Tr}\left(\mathbf{W}_0\mathbf{H}\right)}{q+\sigma^2}\right)\right\} \quad (20)$$

$$e_{10} = e_s + \mathrm{Tr}\left(\mathbf{W}_0\right)\left(\Omega T - \tau\right) \quad (21)$$

$$R_{11} = \frac{1}{\Omega T}\left\{\left[E(X_0)_{busy}T\right]\log_2\left(1+\frac{\mathrm{Tr}\left(\mathbf{W}_1\mathbf{H}\right)}{\sigma^2}\right)\right. \left. + \left(\Omega - E(X_0)_{busy} - \frac{\tau}{T}\right)T\log_2\left(1+\frac{\mathrm{Tr}\left(\mathbf{W}_1\mathbf{H}\right)}{q+\sigma^2}\right)\right\} \quad (22)$$

$$e_{11} = e_s + \mathrm{Tr}\left(\mathbf{W}_1\right)\left(\Omega T - \tau\right). \quad (23)$$

It is worth noting that e_s can be ignored as it is generally very small compared to the energy cost for data transmission.

The average throughput and, the average energy cost of the CBS per slot and the average interference to the MUEs when the spectrum sensing interval is Ω are given as

$$R_{ave} = P\left(H_0^n\right)\left(1-P_f\left(e_s\right)\right)R_{00} + P\left(H_0^n\right)P_f\left(e_s\right)R_{01} + P\left(H_1^n\right)\left(1-\overline{P}_d\right)R_{10} + P\left(H_1^n\right)\overline{P}_dR_{11} \quad (24)$$

$$e_{ave} = \frac{1}{\Omega}\left[P\left(H_0^n\right)\left(1-P_f\left(e_s\right)\right)e_{00} + P\left(H_0^n\right)P_f\left(e_s\right)e_{01} + P\left(H_1^n\right)\left(1-\overline{P}_d\right)e_{10} + P\left(H_1^n\right)\overline{P}_de_{11}\right] \quad (25)$$

$$I_{ave,j} = c_1\mathrm{Tr}\left(\mathbf{W}_0\mathbf{U}_j\right) + c_2\mathrm{Tr}\left(\mathbf{W}_1\mathbf{U}_j\right) + c_3\mathrm{Tr}\left(\mathbf{W}_0\mathbf{U}_j\right) + c_4\mathrm{Tr}\left(\mathbf{W}_1\mathbf{U}_j\right), \quad j = 1, 2, \ldots, J \quad (26)$$

where $P\left(H_0^n\right)$ and $P\left(H_1^n\right)$ are the probabilities of idle status and busy status of the MBS at slot n, respectively. c_1, c_2, c_3 and c_4 are given as

$$c_1 = P\left(H_0^n\right)\left(1-P_f\left(e_s\right)\right)\frac{\left(\Omega - E(X_0)_{idle}\right)}{\Omega} \quad (27)$$

$$c_2 = P\left(H_0^n\right)P_f\left(e_s\right)\frac{\left(\Omega - E(X_0)_{idle}\right)}{\Omega} \quad (28)$$

$$c_3 = P\left(H_1^n\right)\left(1-\overline{P}_d\right)\frac{\left(\Omega - E(X_0)_{busy} - \frac{\tau}{T}\right)}{\Omega} \quad (29)$$

$$c_4 = P\left(H_1^n\right)\overline{P}_d\frac{\left(\Omega - E(X_0)_{busy} - \frac{\tau}{T}\right)}{\Omega}. \quad (30)$$

A. CBS THROUGHPUT MAXIMIZATION

We first investigate the CBS throughput maximization problem subject to the secrecy rate constraint, energy harvesting constraints, MUEs interference power constraints and the CBS transmit power constraint. The problem is given as

$$\boldsymbol{P}_1: \max_{\mathbf{W_0},\mathbf{W_1},\tau,\Omega} R_{ave} \quad (31a)$$
$$\text{s.t. } C1: I_{ave,j} \le I_{th}^{(j)},\ j \in \ell \quad (31b)$$
$$C2: \mathrm{Tr}\left(\mathbf{W}_i\right) \le P_{\max},\ i = 0, 1 \quad (31c)$$
$$C3: 0 < \tau \le T \quad (31d)$$
$$C4: 1 \le \Omega \le \Omega_{\max} \quad (31e)$$
$$C5: \frac{\frac{M_k}{1+\exp\left(-a_k\left(P_{ER_k}-b_k\right)\right)} - M_kZ_k}{1-Z_k} \ge \psi_k \quad (31f)$$
$$i = 0, 1,\ k \in \kappa$$
$$C6: \mathbf{W}_i \succeq 0, i = 0, 1 \quad (31g)$$
$$C7: \mathrm{Rank}\left(\mathbf{W}_i\right) = 1, i = 0, 1 \quad (31h)$$
$$C8: \frac{\mathrm{Tr}\left(\mathbf{W}_i\mathbf{G}_k\right)}{\sigma^2} \le \Upsilon_k,\ i = 0, 1,\ k \in \kappa. \quad (31i)$$

where $I_{th}^{(j)}$ is the maximum tolerable interference power of the ith MUE; $P_{\max}$ is the maximum transmit power of the CBS; ψ_k and Υ_k are the minimum harvesting energy required and the maximum received SNR of the CBS signal at the kth EHR, respectively. In (31b)-(31h), C1 guarantee the QoS of the MUEs; C2 limits the transmit power of the CBS; C3 and C4 limit the sensing time and the sensing interval, respectively. C5 is the energy harvesting constraints. Υ_k is the minimum secrecy SNR which prevents the EHRs from decoding the information send to the CUE. $\mathbf{P}_1$ is non-convex due to the non-convex constraints C3, C4 and C7. The optimal Ω and τ can be obtained by using a one-dimensional line search method. C7 can be relaxed by using semidefinite relaxation (SDR). Given Ω and τ, $\mathbf{P_1}$ can be transformed into the following problem

$$\boldsymbol{P}_2: \max_{\mathbf{W}_0,\mathbf{W}_1,\boldsymbol{\vartheta}} R_{ave} \quad (32a)$$
$$\text{s.t. } C1, C2, C6, C8 \quad (32b)$$
$$C5a: \frac{M_j}{1+\exp\left(-a_k\left(\vartheta_k - b_k\right)\right)} \ge \psi_k\left(1-Z_k\right) + M_kZ_k,\ i = 0, 1,\ k \in \kappa \quad (32c)$$
$$C5b: \mathrm{Tr}\left(\mathbf{W}_i\mathbf{G}_k\right) \ge \vartheta_k,\ i = 0, 1,\ k \in \kappa \quad (32d)$$
$$C5c: \vartheta_k \ge 0,\ k \in \kappa. \quad (32e)$$

where $\boldsymbol{\vartheta} = \{\vartheta_k\}_{k=1}^K$ are slack variables. It can be seen that $\mathbf{P}_2$ is convex and can be solved by the software CVX. If the rank of $\mathbf{W}_0$ and $\mathbf{W}_1$ are not one, Gaussian randomization procedure can be used to obtain a suboptimal solution [41].

Theorem 1: If $\omega_i^* > 0, i = 0, 1$ and $Tr\left(\mathbf{W}_i\mathbf{G}_k\right) > \vartheta_k, i = 0, 1, k \in \kappa$, the optimal $\mathbf{W}_i, i = 0, 1$ of $\mathbf{P}_2$ are rank-one, where $\omega_i^*, i = 0, 1$ are the Lagrangian multipliers corresponding to constraint C2 when $i = 0, 1$.

Proof: Please refer to Appendix A. ■

The optimal Ω and τ can be obtained by searching from $[1, \Omega_{\max}]$ and $(0, T]$, respectively. Then, Algorithm 1 is proposed to solve $\mathbf{P}_1$, which is summarized in Table 1. Table 2 shows the Gaussian randomization procedure for problem $\mathbf{P}_2$.

TABLE 1. **The two-dimensional line search algorithm.**

Algorithm 1: The two-dimensional line search algorithm

1: **Inputting:**
$I_{th}^{(j)}, j \in \ell$, $P_{\max}$, $\psi_k, k \in \kappa$,
$\vartheta_k, k \in \kappa$, $\Upsilon_k, k \in \kappa$.
2: **Initialization:**
the iteration index n=1.
3: **Optimization:**
for $\Omega = 1 : 1 : \Omega_{\max}$
  for $\tau = \Delta\tau : \Delta\tau : T$
   use software CVX to solve $\mathbf{P_2}$;
   obtain $\mathbf{W}_i^n, i = 0, 1$;
   if Rank $\left(\mathbf{W_i^n}\right) = 1, \mathrm{i} = 0, 1$
    calculate the optimal solution R_{ave}^n.
   else
   use Gaussian randomization procedure to obtain the suboptimal solution R_{ave}^n.
   end
  end
end
4: **Comparison:**
compare all R_{ave}^n and obtain the optimal $\mathbf{W_i^*}, i = 0, 1$, τ^* and Ω^*;

TABLE 2. **Gaussian randomization procedure for problem $\mathbf{P_2}$.**

Given:
Given a number of randomizations L, an optimal solution $\mathbf{W}_i, i = 0, 1$ of $\mathbf{P}_2$.
Step 1:
Generate L random vectors $\boldsymbol{\omega}_i^{(l)}, l = 1, \ldots, L$ from $\mathcal{CN}\left(\mathbf{0}, \mathbf{W}_i\right), i = 0, 1$.
Step 2:
For $l = 1, \ldots, L$, let $\mathbf{u}_i^{(l)} = \frac{\boldsymbol{\omega}_i^{(l)}}{\left\|\boldsymbol{\omega}_i^{(l)}\right\|}, i = 0, 1$,
substitute $\mathbf{W}_i^{(l)} = p_i \mathbf{u}_i^{(l)} \left(\mathbf{u}_i^{(l)}\right)^H, i = 0, 1$ into $\mathbf{P}_2$ and optimize $p_i \geq 0, i = 0, 1$. For each l, let $P^{(l)}$ be the optimal value.
Step 3:
Let $l^* = \arg\min_{l=1,\ldots,L} P^{(l)}$ and output
$\mathbf{W}_i^{l*} = p_i \mathbf{u}_i^{(l*)} \left(\mathbf{u}_i^{(l*)}\right)^H$, $i = 0, 1$ as an approximate solution to $\mathbf{P}_2$.

B. ENERGY COST OF THE CBS MINIMIZATION

In this subsection, a resource allocation scheme is studied to minimize the energy cost of the CBS, while guaranteeing that the average throughput of the CBS is above the lower limit R_{req}, which is given as follows

$$\boldsymbol{P}_3: \min_{\mathbf{W}_0, \mathbf{W}_1, \tau, \Omega} \; e_{ave} \tag{33a}$$
$$\text{s.t. } C1, C2, C3, C4, C5, C6, C7, C8 \tag{33b}$$
$$C9: R_{ave} \geq R_{req}. \tag{33c}$$

Following the similar procedure in subsection A, $\mathbf{P}_3$ can be translated into $\mathbf{P}_4$ based on the SDR for given τ and Ω, which is given as

$$\boldsymbol{P}_4: \min_{\mathbf{W}_0, \mathbf{W}_1, \boldsymbol{\vartheta}} \; e_{ave} \tag{34a}$$
$$\text{s.t. } C1, C2, C5a, C5b, C5c, C6, C8, C9. \tag{34b}$$

where R_{req} is the required throughput of the CBS. $\mathbf{P}_4$ is convex and can be solved by using CVX. If the rank of $\mathbf{W}_0$ and $\mathbf{W}_1$ are not one, the Gaussian randomization procedure can be used to obtain a suboptimal solution.

Theorem 2: The optimal $\mathbf{W}_i$, $i = 0, 1$ of $\mathbf{P}_4$ are rank-one, if $o_i^* > 0, i = 0, 1$ and $\theta_{k,i}^{(1*)} = 0, i = 0, 1, k \in \kappa$ or $o_i^* = 0, i = 0, 1$ and only one of $\theta_{k,i}^{(1*)}, k \in \kappa$ is not equal to 0 for a given i, where $\theta_{k,i}^{(1*)} = 0, i = 0, 1, k \in \kappa$ and $o_i^*, i = 0, 1$ are the Lagrangian multipliers corresponding to constraints C5b and C9 when i = 0, 1, respectively.

Proof: Please refer to Appendix B. ∎

The problem $\mathbf{P}_3$ can be solved by Algorithm 1 with slight modification.

C. INTERFERENCE TO THE MUEs MINIMIZATION

The optimization problems in Subsection A and B are mainly from the viewpoints of the CBS. In this subsection we formulate an optimization problem to minimize the interferences to the MUEs, which is from the viewpoint of the MUEs. The problem is given as

$$\boldsymbol{P}_5: \min_{\mathbf{W}_0, \mathbf{W}_1, \tau, \Omega} \; \sum_{j=1}^{J} I_{ave,j} \tag{35a}$$
$$\text{s.t. } C2, C3, C4, C5, C6, C7, C8, C9. \tag{35b}$$

Following the similar procedure in subsection A and B, $\mathbf{P}_5$ can be translated into $\mathbf{P}_6$ based on the SDR for given τ and Ω, which is given as

$$\boldsymbol{P}_6: \min_{\mathbf{W}_0, \mathbf{W}_1, \boldsymbol{\vartheta}} \; \sum_{j=1}^{J} I_{ave,j} \tag{36a}$$
$$\text{s.t. } C2, C5a, C5b, C5c, C6, C8, C9. \tag{36b}$$

$\mathbf{P}_6$ is convex and can be solved by using CVX. If the rank of $\mathbf{W}_0$ and $\mathbf{W}_1$ are not one, the Gaussian randomization procedure can be used to obtain a suboptimal solution. The problem $\mathbf{P}_5$ can be solved by Algorithm 1 with slight modification.

Theorem 3: The optimal $\mathbf{W}_i$, $i = 0, 1$ of $\mathbf{P}_6$ are rank-one, if $\omega_i^{(2*)} > 0, i = 0, 1$ and $o_i^{(1*)} > 0, i = 0, 1$, $\theta_{k,0}^{(2*)} = 0$, $k \in \kappa$ or $o_i^{(1*)} = 0, i = 0, 1$ and only one of $\theta_{k,i}^{(2*)}, k \in \kappa$ is not equal to 0 for a given i, where $\omega_i^{(2*)}, \theta_{k,i}^{(2*)} i = 0, 1$ and o_i^*, $i = 0, 1, k \in \kappa$ are the Lagrangian multipliers corresponding to constraint C2, C5b, and C8 when i = 0, 1, respectively.

Proof: Please refer to Appendix C. ∎

D. COMPLEXITY ANALYSIS

Recall that the problems $\mathbf{P}_2$, $\mathbf{P}_4$ and $\mathbf{P}_6$ are convex and can be solved by interior-point method [42]. Similar to [43],

TABLE 3. Complexity analysis.

Problem	Complexity Order
CBS Throughput Maximization	$T_1\sqrt{2N_t+J+7K+2}\cdot n\cdot\left[2+J+7K+2N_t^3+n\left(2+J+7K+2N_t^2\right)+n^2\right]$
Energy Cost of the CBS Minimization	$T_1\sqrt{2N_t+7K+3}\cdot n\cdot\left[3+7K+2N_t^3+n\left(3+7K+2N_t^2\right)+n^2\right]$
Interference to the MUEs Minimization	$T_1\sqrt{2N_t+7K+3}\cdot n\cdot\left[3+7K+2N_t^3+n\left(3+7K+2N_t^2\right)+n^2\right]$

TABLE 4. Simulation parameters.

Parameter	Value
Maximum transmit power of the CBS P_{max}	10 dBW
Maximum tolerable interference power I_{th}	-10 dBm
Number of the EHRs K	3
Number of the MUEs J	4
The length of a slot T	100ms
Path-loss exponent α	2
Distances d_{IR}, d_{ER_k} and d_{MUE_j}	30m, 20m, 20m
Channel gains	$\mathbf{h}_{IR}\sim\mathcal{CN}\left(0,2\mathbf{I}\right)$, $\mathbf{g}_{ER_k}\sim\mathcal{CN}\left(0,2\mathbf{I}\right),\ k\in\kappa$, $\mathbf{u}_{MUE_j}\sim\mathcal{CN}\left(0,1\mathbf{I}\right),\ j\in\ell$
Maximum spectrum sensing interval $\Omega_{\max}$	3
Variances of noise	10 dBm
Non-linear EH parameters M_k, a_k, b_k	20 mW, 6400, 0.003 [38]
Maximum received SNR of the CBS signal Υ_k	5 dB
Minimum harvesting energy ψ_k	10 dBm
Received MBS signal strength at the CUE q	20 dBm
Transmission matrix $\boldsymbol{A}$	$\begin{bmatrix}0.7 & 0.3\\ 0.4 & 0.6\end{bmatrix}$

we can use the computational complexity of interior-point method to measure the complexity of the proposed algorithm. The computational complexity of interior-point method is related to the number of linear matrix inequalities and second-order cone constraints. According to [43], the complexity of Algorithm 1 is given in Table 3, where $T_1 = \Omega_{\max}\frac{T}{\Delta\tau}$, $n = O\left(2N_t^2\right)$ and $O\left(\cdot\right)$ is the big-O notation. Indeed, the complexity of the proposed algorithm is relatively high. However, the optimization problems are solved in the CBS, which has strong computational capability. Moreover, the spectrum sensing time τ has relatively fewer impacts on the optimal value, the complexity can be reduced by fixing the spectrum sensing time τ.

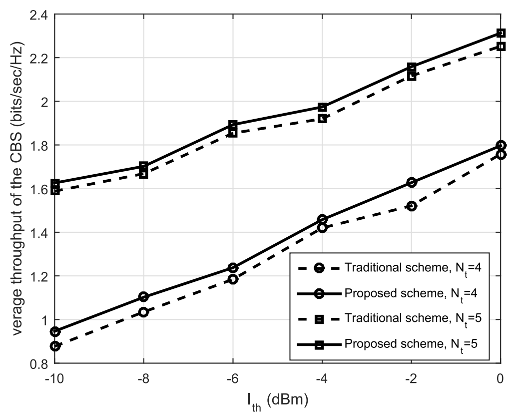

FIGURE 3. Average throughput of the CBS versus I_{th} in problem $\mathbf{P}_1$.

IV. SIMULATION RESULTS

In this section, simulation results are provided to evaluate the performance of the proposed algorithms. The simulation parameters for the numerical results are summarized in Table 3, which are set without loss of generality. We assume flat-fading channels with path-loss and Rayleigh fading, $|\mathbf{h}|^2 = d_{IR}^{-\alpha}|\mathbf{h}_{IR}|^2$, $|\mathbf{g}_k|^2 = d_{ER_k}^{-\alpha}\left|\mathbf{g}_{ER_k}\right|^2, k\in\kappa$ and $\left|\mathbf{u}_j\right|^2 = d_{MUE_j}^{-\alpha}\left|\mathbf{u}_{MUE_j}\right|^2, j\in\ell$, where d_{IR}, d_{ER_k} and d_{MUE_j} are the distance from the CBS to the CUE, the kth EHR and jth MUEs, respectively. α is the path-loss exponent. $\mathbf{h}_{IR}$, $\mathbf{g}_{ER_k}$ and $\mathbf{u}_{MUE_j}$ follow Gaussian distribution which are shown in Table 4.

Fig. 3 shows the average throughput of the CBS versus the interference limits $I_{th}^{(j)}$ in problem $\mathbf{P}_1$. For convenience, we set all $I_{th}^{(j)}$ equal to I_{th} which ranges from -10 dBm to 0 dBm. It is seen that the average throughput of the CBS increases with the I_{th}. A larger I_{th} implies that the MUEs can tolerate more interferences from the CBS, which allows the CBS to use a larger transmit power or larger spectrum sensing interval. Another phenomenon that can be found in Fig. 3 is that our proposed algorithm can achieve about higher average throughput of the CBS than the traditional spectrum sensing scheme, i.e, $\Omega_{\max} = 1$. It matches our discussion in Section I-A that the statistical property of the MBS can be used to gain higher throughput of the CBS. Finally, it can be seen in Fig. 3 that the average throughput of the CBS increases with the number of the transmit antennas of the CBS. The reason if that a larger value of N_t enlarges the feasible region of optimization problem $\mathbf{P}_1$.

Fig. 4 displays the average spectrum sensing interval of the CBS versus I_{th} in problem $\mathbf{P}_1$. As shown in Fig. 4, the average spectrum sensing interval increases with I_{th} and N_t. A smaller value of I_{th} implies that the protection requirements of the

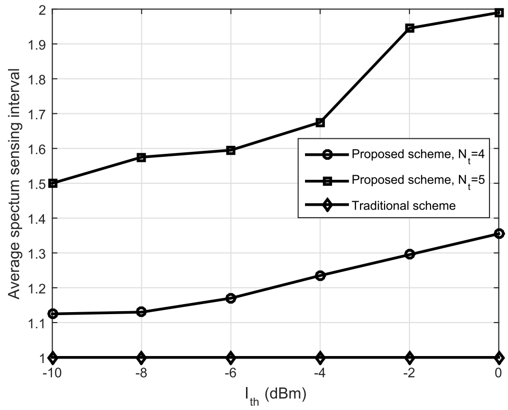

FIGURE 4. **Average spectrum sensing interval versus I_{th} in problem $\mathbf{P}_1$.**

MUEs is high, hence, the CBS must sense the status of the MBS frequently, i.e., adopts smaller spectrum sensing interval. An increase of the N_t increases the degrees of freedom of the spectrum sensing interval.

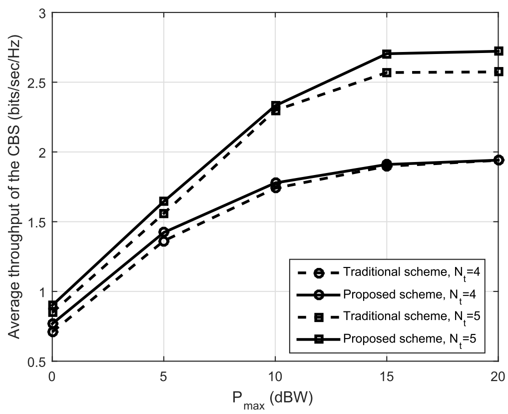

FIGURE 5. **Average throughput of the CBS versus P_{max} in problem $\mathbf{P}_1$.**

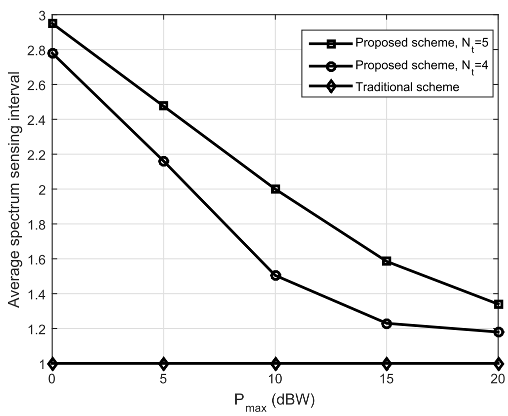

FIGURE 6. **Average spectrum sensing interval of the CBS versus P_{max} in problem $\mathbf{P}_1$.**

Fig. 5 and Fig. 6 show the trend of the average throughput and the spectrum sensing interval of the CBS versus the maximum transmit power limit P_{max} in $\mathbf{P}_1$. It can be seen from Fig. 5 and Fig. 6 that the average throughput and the spectrum sensing interval of the CBS increase with P_{max} and N_t. Similar to Fig. 3 and Fig. 4, this is because that larger P_{max} and N_t enlarge the feasible region of optimization problem $\mathbf{P}_1$.

Fig. 7 displays average energy cost of the CBS versus R_{req} in problem $\mathbf{P}_3$. In Fig. 7, the average energy cost of the CBS increases when R_{req} increases from 0.5 bps to 2.5 bps. In order to meet the increase of the minimum throughput of the CBS requirement R_{req}, the CBS must increase its transmit power, which may increase the average energy cost of the CBS. According to Fig. 7, Fig. 8 and Fig.9, it can been seen that the CBS will adopt larger transmit power and spectrum sensing interval to meet the throughput constraint C9.

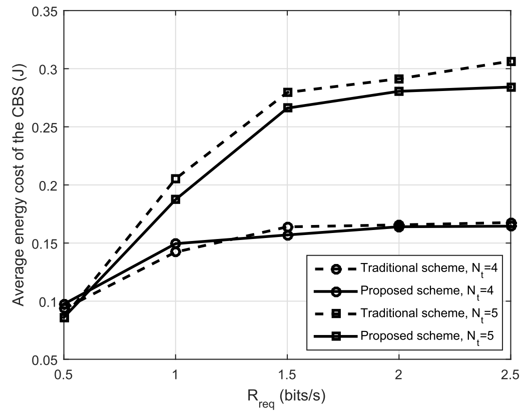

FIGURE 7. **Average energy cost of the CBS versus R_{req} in problem $\mathbf{P}_1$.**

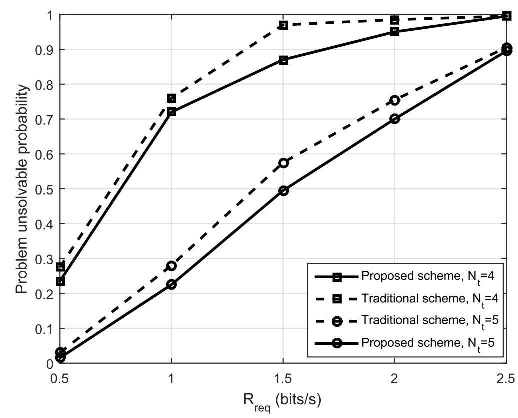

FIGURE 8. **Problem $\mathbf{P}_3$ unsolvable probability versus R_{req}.**

Fig. 8 shows the problem unsolvable probability versus R_{req} in $\mathbf{P}_3$. The problem unsolvable probability is defined as the probability that the of problem $\mathbf{P}_3$ is unsolvable, or the probability that there are no feasible solutions of $\mathbf{P}_3$. It can be seen from Fig. 8 that the problem unsolvable probabilities of the proposed algorithm are lower than the traditional spectrum sensing scheme. The reason is that when R_{req} becomes large and the channel qualities become worse, the traditional spectrum sensing scheme can not find feasible solutions due to the constraints C1 and C9. On the other hand, by using the proposed spectrum sensing scheme, the CBS can use lager spectrum sensing interval to satisfy the constraint C9. Therefore, our proposed algorithm has greater dynamic range than the traditional spectrum sensing scheme, which matches our discussion in Section I-A. Finally, it can be seen that the unsolvable probability decreases with N_t. It can be explained by the fact that a larger N_t can provide much more degrees of freedom of the beamforming matrix.

Fig. 9 illustrates the average spectrum sensing interval versus R_{req} in problem $\mathbf{P}_3$. As shown in Fig. 9, the average spectrum sensing interval increases with R_{req}, which coincides with our intuition that the CBS has to use larger spectrum sensing interval to satisfy the increased R_{req}. Meanwhile, we can observe that the average spectrum sensing interval decreases with N_t, which indicates that the CBS satisfies the minimum throughput constraint mainly through adjusting the beamforming matrix.

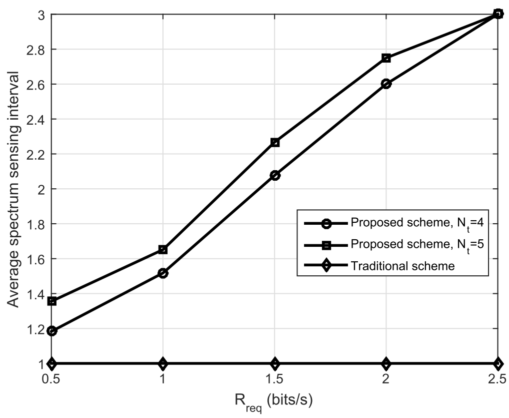

FIGURE 9. Average spectrum sensing interval versus the R_{req} in problem $\mathbf{P}_3$.

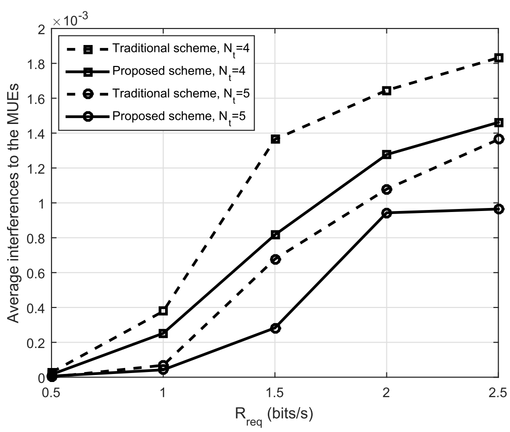

FIGURE 10. The average interference caused to MUEs versus R_{req} in problem $\mathbf{P}_5$.

Fig. 10 shows the average interferences to the MUEs versus R_{req} in problem $\mathbf{P}_5$. It can be seen from Fig. 10 that the average interferences to the MUEs increase with R_{req}. The reason is that the CBS uses larger transmit power to meet the minimum throughput constraint, which may introduce more interferences to the MUEs. As shown in Fig. 10 that increasing N_t could mitigate the interferences to the MUEs, which is because that larger N_t provides more degrees of freedom of the problem $\mathbf{P}_5$.

Fig. 11 shows the unsolvable probability of problem $\mathbf{P}_5$ versus R_{req}. It can be seen from Fig. 11 that the problem unsolvable probability of the proposed algorithm is lower than the traditional spectrum sensing scheme. Moreover, the unsolvable probability decreases with N_t. The reason for these phenomena are similar to that of Fig. 8. Therefore, our proposed algorithm has greater dynamic range than the traditional spectrum sensing, which matches our discussion in Section I-A.

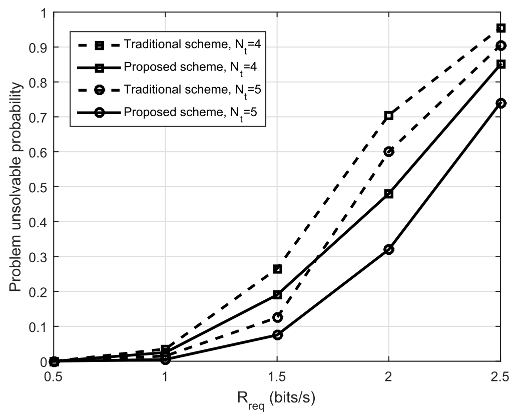

FIGURE 11. Problem $\mathbf{P}_5$ unsolvable probability versus R_{req}.

V. CONCLUSION

In this paper, we considered a cognitive small cell network, which can be applied into 5G systems. Three optimization problems were formulated such as the CBS throughput maximization problem, the energy cost of the CBS minimization problem and the interference to the MUEs minimization problems. An algorithm based on the one-dimensional line search method, SDR and CVX was proposed to solve these problems. Three theorems were derived to given the conditions that the three problem had rank-one solutions. Simulation results showed that the proposed algorithm has higher throughput of the CBS and larger dynamic range than the traditional spectrum sensing scheme.

APPENDIX A
PROOF OF THEOREM 1

The Lagrangian related with $\mathbf{W}_0$ in problem $\mathbf{P_2}$ is given by

$$L_1 = -l_1 \log_2\left(1+\frac{\mathrm{Tr}\left(\mathbf{W}_0\mathbf{H}\right)}{\sigma^2}\right) - l_2 \log_2\left(1+\frac{\mathrm{Tr}\left(\mathbf{W}_0\mathbf{H}\right)}{q+\sigma^2}\right) + \sum_{j=1}^{J}\lambda_j\left[c_1\mathrm{Tr}\left(\mathbf{W}_0\mathbf{U}_j\right)+c_3 Tr\left(\mathbf{W}_0\mathbf{U}_j\right)\right]+\omega_0\mathrm{Tr}\left(\mathbf{W}_0\right)$$

$$- \sum_{k=1}^{K} \theta_{k,0} \mathrm{Tr}\left(\mathbf{W}_0 \mathbf{G}_k\right) - \mathrm{Tr}\left(\mathbf{W}_0 \mathbf{Z}_0\right) + \sum_{k=1}^{K} \varpi_{k,0} \mathrm{Tr}\left(\mathbf{W}_0 \mathbf{G}_k\right) + \Delta \quad (37)$$

where $\lambda_j \geq 0, j \in \ell$, $\omega_0 \geq 0$, $\theta_{k,0} \geq 0, k \in \kappa$, $\mathbf{Z}_0 \succeq 0$, $\varpi_{k,0} \geq 0, k \in \kappa$ are the dual variables with respect to C1, C2, C5b and C8, respectively. Δ is a collection of variables and constants that are not relevant to the proof. l_1 and l_2 are given by

$$l_1 = P\left(H_0^n\right)\left(1 - P_f\left(e_s\right)\right) \frac{1}{\Omega T}\left[E(X_0)_{idle} T - \tau\right] + P\left(H_1^n\right)\left(1 - \overline{P}_d\right) \frac{1}{\Omega T} E(X_0)_{busy} T \quad (38)$$

$$l_2 = P\left(H_0^n\right)\left(1 - P_f\left(e_s\right)\right) \frac{1}{\Omega T}\left(\Omega - E(X_0)_{idle}\right) T + P\left(H_1^n\right)\left(1 - \overline{P}_d\right) \frac{1}{\Omega T}\left(\Omega - E(X_0)_{busy} - \frac{\tau}{T}\right) T. \quad (39)$$

The partial Karush-Kuhn-Tucker (KKT) optimality conditions related to our proof are given as follows:

$$- \frac{l_1}{\ln 2\left[\sigma^2 + \mathrm{Tr}\left(\mathbf{W}_0^* \mathbf{H}\right)\right]} \mathbf{H} - \frac{l_2}{\ln 2\left[q + \sigma^2 + \mathrm{Tr}\left(\mathbf{W}_0^* \mathbf{H}\right)\right]} \mathbf{H} + \sum_{j=1}^{J} \lambda_j^* \left(c_1 + c_3\right) \mathbf{U}_j + \omega_0^* \mathbf{I} - \sum_{k=1}^{K} \theta_{k,0}^* \mathbf{G}_k - \mathbf{Z}_0^* + \sum_{k=1}^{K} \varpi_{k,0}^* \mathbf{G}_k = 0 \quad (40)$$

$$\mathbf{W}_0^* \mathbf{Z}_0^* = 0 \quad (41)$$

$$\lambda_j^* \geq 0, \omega_0^* \geq 0, \theta_{k,0}^* \geq 0, \mathbf{Z}_0^* \succeq 0, \varpi_{k,0}^* \geq 0. \quad (42)$$

Then through some algebraic operations, we have

$$\sum_{j=1}^{J} \lambda_j^* \left(c_1 + c_3\right) \mathbf{U}_j + \omega_0^* \mathbf{I} + \sum_{k=1}^{K} \varpi_{k,0}^* \mathbf{G}_k = \frac{l_1}{\ln 2\left[\sigma^2 + \mathrm{Tr}\left(\mathbf{W}_0^* \mathbf{H}\right)\right]} \mathbf{H} + \frac{l_2}{\ln 2\left[q + \sigma^2 + \mathrm{Tr}\left(\mathbf{W}_0^* \mathbf{H}\right)\right]} \mathbf{H} + \sum_{k=1}^{K} \theta_{k,0}^* \mathbf{G}_k + \mathbf{Z}_0^* \quad (43)$$

We multiply the both sides of (43) by $\mathbf{W}_0^*$ leading to

$$\mathbf{W}_0^* \left[\sum_{j=1}^{J} \lambda_j^* \left(c_1 + c_3\right) \mathbf{U}_j + \omega_0^* \mathbf{I} + \sum_{k=1}^{K} \varpi_{k,0}^* \mathbf{G}_k\right] = \mathbf{W}_0^* \left\{\frac{l_1}{\ln 2\left[\sigma^2 + \mathrm{Tr}\left(\mathbf{W}_0^* \mathbf{H}\right)\right]} \mathbf{H} + \frac{l_2}{\ln 2\left[q + \sigma^2 + \mathrm{Tr}\left(\mathbf{W}_0^* \mathbf{H}\right)\right]} \mathbf{H} + \sum_{k=1}^{K} \theta_{k,0}^* \mathbf{G}_k\right\} \quad (44)$$

If $\omega_0^* > 0$, $\theta_{k,0}^* = 0$, then one has

$$\sum_{j=1}^{J} \lambda_j^* \left(c_1 + c_3\right) \mathbf{U}_j + \omega_0^* \mathbf{I} + \sum_{k=1}^{K} \varpi_{k,0}^* \mathbf{G}_k \succ 0 \quad (45)$$

$$\mathrm{Rank}\left(\mathbf{W}_0^*\right) = \mathrm{Rank}\left\{\mathbf{W}_0^* \left[\frac{l_1}{\ln 2\left[\sigma^2 + \mathrm{Tr}\left(\mathbf{W}_0^* \mathbf{H}\right)\right]} + \frac{l_2}{\ln 2\left[q + \sigma^2 + \mathrm{Tr}\left(\mathbf{W}_0^* \mathbf{H}\right)\right]}\right] \mathbf{H}\right\} \leq \min\left\{\mathrm{Rank}\left(\mathbf{W}_\mathbf{0}^*\right), \mathrm{Rank}\left(\mathbf{H}\right)\right\} = 1 \quad (46)$$

Since $\mathbf{W}_0^* \neq 0$, the rank of $\mathbf{W}_\mathbf{0}^*$ is one. The proof of the $\mathbf{W}_1^*$ is similar to the case of $\mathbf{W}_0^*$. The proof is competed.

APPENDIX B
PROOF OF THEOREM 2

The Lagrangian related with $\mathbf{W}_0$ of problem $\mathbf{P}_4$ is given as

$$L_2 = \mathrm{Tr}\left(\mathbf{W}_0\right) d_1 + \sum_{j=1}^{J} \lambda_j^{(1)} \left[c_1 \mathrm{Tr}\left(\mathbf{W}_0 \mathbf{U}_j\right) + c_3 \mathrm{Tr}\left(\mathbf{W}_0 \mathbf{U}_j\right)\right] + \omega_0^{(1)} \mathrm{Tr}\left(\mathbf{W}_0\right) - \sum_{k=1}^{K} \theta_{k,0}^{(1)} \mathrm{Tr}\left(\mathbf{W}_0 \mathbf{G}_k\right) - \mathrm{Tr}\left(\mathbf{W}_0 \mathbf{Z}_0^{(1)}\right) + \sum_{k=1}^{K} \varpi_{k,0}^{(1)} \mathrm{Tr}\left(\mathbf{W}_0 \mathbf{G}_k\right) - o_0 \left\{\frac{l_1}{\ln 2\left[\sigma^2 + \mathrm{Tr}\left(\mathbf{W}_0^* \mathbf{H}\right)\right]} + \frac{l_2}{\ln 2\left[q + \sigma^2 + \mathrm{Tr}\left(\mathbf{W}_0^* \mathbf{H}\right)\right]}\right\} \mathbf{H} + \Delta \quad (47)$$

where $\lambda_j^{(1)} \geq 0, j \in \ell$, $\omega_0^{(1)} \geq 0$, $\theta_{k,0}^{(1)} \geq 0, k \in \kappa$, $\mathbf{Z}_0^{(1)} \succeq 0$, $\varpi_{k,0}^{(1)} \geq 0, k \in \kappa$, $o_0 \geq 0$ are the dual variables with respect to C1, C2, C5b, C6, C8 and C9, respectively. Δ is a collection of variables and constants that are not relevant to the proof. d_1 is given as

$$d_1 = \left[P\left(H_0^n\right)\left(1 - P_f\left(e_s\right)\right) + P\left(H_1^n\right)\left(1 - \overline{P}_d\right)\right] \times \left(\frac{\Omega T - \tau}{\Omega}\right) \quad (48)$$

Following the similar proof process of Appendix A, we have

$$\mathbf{W}_0^* \left[d_1 \mathbf{I} + \sum_{j=1}^{J} \lambda_j^{(1*)} \left(c_1 + c_3\right) \mathbf{U}_j + \omega_0^{(1*)} \mathbf{I} + \sum_{k=1}^{K} \varpi_{k,0}^{(1)} \mathbf{G}_k\right] = \mathbf{W}_0^* \left\{\sum_{k=1}^{K} \theta_{k,0}^{(1*)} \mathbf{G}_k + o_0^* \left\{\frac{l_1}{\ln 2\left[\sigma^2 + \mathrm{Tr}\left(\mathbf{W}_0^* \mathbf{H}\right)\right]} + \frac{l_2}{\ln 2\left[q + \sigma^2 + \mathrm{Tr}\left(\mathbf{W}_0^* \mathbf{H}\right)\right]}\right\} \mathbf{H}\right\} \quad (49)$$

Refer to (46), it can be seen form (49) that, if $o_0^* > 0$ and $\theta_{k,0}^{(1*)} = 0, k \in \kappa$ or $o_0^* = 0$ and only one of $\theta_{k,0}^{(1*)}, k \in \kappa$ is not equal to 0, $\mathrm{Rank}\left(\mathbf{W}_0^*\right) = 1$. The proof of the $\mathbf{W}_1^*$ is similar to the case of $\mathbf{W}_0^*$. The proof is competed.

APPENDIX C
PROOF OF THEOREM 3

The Lagrangian related with $\mathbf{W}_0$ in problem $\mathbf{P}_6$ is given as

$$\begin{aligned} L_3 = &\sum_{j=1}^{J}\left[c_1 \mathrm{Tr}\left(\mathbf{W}_0 U_j\right) + c_3 \mathrm{Tr}\left(\mathbf{W}_0 \mathbf{U}_j\right)\right] + \omega_0^{(2)} \mathrm{Tr}\left(\mathbf{W}_0\right) \\ &- \sum_{k=1}^{K} \theta_{k,0}^{(2)} \mathrm{Tr}\left(\mathbf{W}_0 \mathbf{G}_k\right) - \mathrm{Tr}\left(\mathbf{W}_0 \mathbf{Z}_0^{(2)}\right) \\ &+ \sum_{k=1}^{K} \varpi_{k,0}^{(2)} \mathrm{Tr}\left(\mathbf{W}_0 \mathbf{G}_k\right) - o_0^{(1)} \left\{ \frac{l_1}{\ln 2\left[\sigma^2 + \mathrm{Tr}\left(\mathbf{W}_0^* \mathbf{H}\right)\right]} \right. \\ &\left. + \frac{l_2}{\ln 2\left[q + \sigma^2 + \mathrm{Tr}\left(\mathbf{W}_0^* \mathbf{H}\right)\right]} \right\} + \Delta \end{aligned} \tag{50}$$

where $\omega_0^{(2)} \geq 0$, $\omega_0^{(1)} \geq 0$, $\theta_{k,0}^{(2)} \geq 0, k = 1, 2, \ldots, K$, $\mathbf{Z}_0^{(2)} \succeq 0$, $\varpi_{k,0}^{(2)} \geq 0, k = 1, 2, \ldots, K$, $o_0^{(1)} \geq 0$ are the dual variables with respect to C2, C5b, C6, C8 and C9, respectively. Δ is a collection of variables and constants that are not relevant to the proof.

Following the similar proof process of Appendix A and B, we have

$$\begin{aligned} &\mathbf{W}_0^* \left(\sum_{j=1}^{J} \left(c_1 + c_3\right) \mathbf{U}_j + \omega_0^{(2*)} \mathbf{I} + \sum_{k=1}^{K} \varpi_{k,0}^{(2*)} \mathbf{G}_k \right) \\ &= \mathbf{W}_0^* \left\{ \sum_{k=1}^{K} \theta_{k,0}^{(2*)} \mathbf{G}_k + \mathbf{Z}_0^{(2*)} + o_0^{(1*)} \right. \\ &\left. \left[\frac{l_1}{\ln 2\left[\sigma^2 + \mathrm{Tr}\left(\mathbf{W}_0^* \mathbf{H}\right)\right]} + \frac{l_2}{\ln 2\left[q + \sigma^2 + \mathrm{Tr}\left(\mathbf{W}_0^* \mathbf{H}\right)\right]} \right] \mathbf{H} \right\}. \end{aligned} \tag{51}$$

Refer to (46), it can be seen form (52) that, if $\omega_0^{(2*)} > 0$ and $o_0^{(1*)} > 0$, $\theta_{k,0}^{(2*)} = 0, k \in \kappa$ or $o_0^{(1*)} = 0$ and only one of $\theta_{k,0}^{(2*)}, k \in \kappa$ is not equal to 0. The proof of the $\mathbf{W}_1^*$ is similar to the case of $\mathbf{W}_0^*$. The proof is competed.

REFERENCES

[1] J. G. Andrews *et al.*, "What will 5G be?" *IEEE J. Sel. Areas Commun.*, vol. 32, no. 6, pp. 1065–1082, Jun. 2014.

[2] H. Zhang, Y. Nie, J. Cheng, V. C. M. Leung, and A. Nallanathan, "Sensing time optimization and power control for energy efficient cognitive small cell with imperfect hybrid spectrum sensing," *IEEE Trans. Wireless Commun.*, vol. 16, no. 2, pp. 730–743, Feb. 2017.

[3] F. H. Tseng, L.-D. Chou, H.-C. Chao, and J. Wang, "Ultra-dense small cell planning using cognitive radio network toward 5G," *IEEE Wireless Commun.*, vol. 22, no. 6, pp. 76–83, Dec. 2015.

[4] C.-X. Wang *et al.*, "Cellular architecture and key technologies for 5G wireless communication networks," *IEEE Commun. Mag.*, vol. 52, no. 2, pp. 122–130, Feb. 2014.

[5] J. Mitola and G. Q. Maguire, "Cognitive radio: Making software radios more personal," *IEEE Pers. Commun.*, vol. 6, no. 4, pp. 13–18, Aug. 1999.

[6] S. Haykin, "Cognitive radio: Brain-empowered wireless communications," *IEEE J. Sel. Areas Commun.*, vol. 23, no. 2, pp. 201–220, Feb. 2005.

[7] F. Zhou, N. C. Beaulieu, Z. Li, J. Si, and P. Qi, "Energy-efficient optimal power allocation for fading cognitive radio channels: Ergodic capacity, outage capacity, and minimum-rate capacity," *IEEE Trans. Wireless Commun.*, vol. 15, no. 4, pp. 2741–2755, Apr. 2016.

[8] F. Zhou, Z. Li, Q. L. J. Cheng, and J. Si, "Robust AN-aided beamforming and power splitting design for secure MISO cognitive radio with SWIPT," *IEEE Trans. Wireless Commun.*, vol. 16, no. 4, pp. 2450–2464, Apr. 2017.

[9] F. Zhou, Z. Li, N. C. Beaulieuz, J. Cheng, and Y. Wang, "Resource allocation in wideband cognitive radio with SWIPT: Max-min fairness guarantees," in *Proc. IEEE Global Commun. Conf. (GLOBECOM)*, Dec. 2016, pp. 1–6.

[10] G. B. Giannakis and M. K. Tsatsanis, "Signal detection and classification using matched filtering and higher order statistics," *IEEE Trans. Acoust., Speech Signal Process.*, vol. 38, no. 7, pp. 1284–1296, Jul. 1990.

[11] X. Zhang, R. Chai, and F. Gao, "Matched filter based spectrum sensing and power level detection for cognitive radio network," in *Proc. IEEE Global Conf. Signal Inf. Process. (GlobalSIP)*, Dec. 2014, pp. 1267–1270.

[12] F. F. Digham, M.-S. Alouini, and M. K. Simon, "On the energy detection of unknown signals over fading channels," *IEEE Trans. Commun.*, vol. 55, no. 1, pp. 21–24, Jan. 2007.

[13] S. P. Herath, N. Rajatheva, and C. Tellambura, "Energy detection of unknown signals in fading and diversity reception," *IEEE Trans. Commun.*, vol. 59, no. 9, pp. 2443–2453, Sep. 2011.

[14] A. Tkachenko, D. Cabric, and R. W. Brodersen, "Cyclostationary feature detector experiments using reconfigurable BEE2," in *Proc. 2nd IEEE Int. Symp. New Frontiers Dyn. Spectr. Access Netw.*, Apr. 2007, pp. 216–219.

[15] M. Bkassiny, S. K. Jayaweera, Y. Li, and K. A. Avery, "Blind cyclostationary feature detection based spectrum sensing for autonomous self-learning cognitive radios," in *Proc. IEEE Int. Conf. Commun. (ICC)*, Jun. 2012, pp. 1507–1511.

[16] S. Sedighi, A. Taherpour, S. Gazor, and T. Khattab, "Eigenvalue-based multiple antenna spectrum sensing: Higher order moments," *IEEE Trans. Wireless Commun.*, vol. 16, no. 2, pp. 1168–1184, Feb. 2017.

[17] Y. Zeng and Y.-C. Liang, "Eigenvalue-based spectrum sensing algorithms for cognitive radio," *IEEE Trans. Commun.*, vol. 57, no. 6, pp. 1784–1793, Jun. 2009.

[18] T. Yucek and H. Arslan, "A survey of spectrum sensing algorithms for cognitive radio applications," *IEEE Commun. Surveys Tuts.*, vol. 11, no. 1, pp. 116–130, 1st Quart., 2009.

[19] X. Y. Wang, P.-H. Ho, and K.-C. Chen, "Interference analysis and mitigation for cognitive-empowered femtocells through stochastic dual control," *IEEE Trans. Wireless Commun.*, vol. 11, no. 6, pp. 2065–2075, Jun. 2012.

[20] H. Zhang, Y. Nie, J. Cheng, V. C. M. Leung, and A. Nallanathan, "Hybrid spectrum sensing based power control for energy efficient cognitive small cell network," in *Proc. IEEE Global Commun. Conf. (GLOBECOM)*, Dec. 2015, pp. 1–5.

[21] S.-M. Cheng, W. C. Ao, F.-M. Tseng, and K.-C. Chen, "Design and analysis of downlink spectrum sharing in two-tier cognitive femto networks," *IEEE Trans. Veh. Technol.*, vol. 61, no. 5, pp. 2194–2207, Jun. 2012.

[22] S. Sardellitti and S. Barbarossa, "Joint optimization of collaborative sensing and radio resource allocation in small-cell networks," *IEEE Trans. Signal Process.*, vol. 61, no. 18, pp. 4506–4520, Sep. 2013.

[23] H. Zhang, C. Jiang, N. C. Beaulieu, X. Chu, X. Wang, and T. Q. S. Quek, "Resource allocation for cognitive small cell networks: A cooperative bargaining game theoretic approach," *IEEE Trans. Wireless Commun.*, vol. 14, no. 6, pp. 3481–3493, Jun. 2015.

[24] R. Urgaonkar and M. J. Neely, "Opportunistic cooperation in cognitive femtocell networks," *IEEE J. Sel. Areas Commun.*, vol. 30, no. 3, pp. 607–616, Apr. 2012.

[25] P. Mach and Z. Becvar, "Energy-aware dynamic selection of overlay and underlay spectrum sharing for cognitive small cells," *IEEE Trans. Veh. Technol.*, vol. 66, no. 5, pp. 4120–4132, May 2017.

[26] R. Xie, F. R. Yu, H. Ji, and Y. Li, "Energy-efficient resource allocation for heterogeneous cognitive radio networks with femtocells," *IEEE Trans. Wireless Commun.*, vol. 11, no. 11, pp. 3910–3920, Nov. 2012.

[27] X. Xing, T. Jing, H. Li, Y. Huo, X. Cheng, and T. Znati, "Optimal spectrum sensing interval in cognitive radio networks," *IEEE Trans. Parallel Distrib. Syst.*, vol. 25, no. 9, pp. 2408–2417, Sep. 2014.

[28] C. Ghosh, C. Cordeiro, D. P. Agrawal, and M. B. Rao, "Markov chain existence and hidden Markov models in spectrum sensing," in *Proc. IEEE Int. Conf. Pervasive Comput. Commun. (PerCom)*, Mar. 2009, pp. 1–6.

[29] D. Treeumnuk and D. C. Popescu, "Using hidden Markov models to evaluate performance of cooperative spectrum sensing," *IET Commun.*, vol. 7, no. 17, pp. 1969–1973, Nov. 2013.

[30] Z. Chen, Z. Hu, and R. C. Qiu, "Quickest spectrum detection using hidden Markov model for cognitive radio," in *Proc. IEEE Military Commun. Conf. (MILCOM)*, Oct. 2009, pp. 1–7.

[31] T. Nguyen, B. L. Mark, and Y. Ephraim, "Spectrum sensing using a hidden bivariate Markov model," *IEEE Trans. Wireless Commun.*, vol. 12, no. 9, pp. 4582–4591, Sep. 2013.
[32] B. Liu, Z. Li, J. Si, and F. Zhou, "Optimal sensing interval in cognitive radio networks with imperfect spectrum sensing," *IET Commun.*, vol. 10, no. 2, pp. 189–198, 2016.
[33] Z. Li, B. Liu, J. Si, and F. Zhou, "Optimal spectrum sensing interval in energy-harvesting cognitive radio networks," *IEEE Trans. Cogn. Commun. Netw.*, vol. 3, no. 2, pp. 190–200, Jun. 2017.
[34] Q. Li, Q. Zhang, and J. Qin, "Secure relay beamforming for SWIPT in amplify-and-forward two-way relay networks," *IEEE Trans. Veh. Technol.*, vol. 65, no. 11, pp. 9006–9019, Nov. 2016.
[35] Q. Li, L. Yang, Q. Zhang, and J. Qin, "Robust AN-aided secure precoding for an AF MIMO untrusted relay system," *IEEE Trans. Veh. Technol.*, vol. 66, no. 11, pp. 10572–10576, Nov. 2017.
[36] E. Boshkovska, D. W. K. Ng, N. Zlatanov, and R. Schober, "Practical non-linear energy harvesting model and resource allocation for SWIPT systems," *IEEE Commun. Lett.*, vol. 19, no. 12, pp. 2082–2085, Dec. 2015.
[37] Y. Wang, Y. Wang, F. Zhou, Y. Wu, and H. Zhou, "Resource allocation in wireless powered cognitive radio networks based on a practical non-linear energy harvesting model," *IEEE Access*, vol. 5, pp. 17618–17626, 2017.
[38] Y. Huang, Z. Li, F. Zhou, and R. Zhu, "Robust AN-aided beamforming design for secure MISO cognitive radio based on a practical nonlinear EH model," *IEEE Access*, vol. 5, pp. 14011–14019, 2017.
[39] Y.-C. Liang, Y. Zeng, E. C. Y. Peh, and A. T. Hoang, "Sensing-throughput tradeoff for cognitive radio networks," *IEEE Trans. Wireless Commun.*, vol. 7, no. 4, pp. 1326–1337, Apr. 2008.
[40] A. Sultan, "Sensing and transmit energy optimization for an energy harvesting cognitive radio," *IEEE Wireless Commun. Lett.*, vol. 1, no. 5, pp. 500–503, Oct. 2012.
[41] Z.-Q. Luo, W.-K. Ma, A. M.-C. So, Y. Ye, and S. Zhang, "Semidefinite relaxation of quadratic optimization problems," *IEEE Signal Process. Mag.*, vol. 27, no. 3, pp. 20–34, May 2010.
[42] A. Ben-Tal, *Lectures on Modern Convex Optimization: Analysis, Algorithms, and Engineering Applications*. Philadelphia, PA, USA: SIAM, 2001.
[43] K.-Y. Wang, A. M.-C. So, T.-H. Chang, W.-K. Ma, and C.-Y. Chi, "Outage constrained robust transmit optimization for multiuser MISO downlinks: Tractable approximations by conic optimization," *IEEE Trans. Signal Process.*, vol. 62, no. 21, pp. 5690–5705, Nov. 2014.

BOYANG LIU received the B.S. and Ph.D. degrees from Xidian University, China, in 2011 and 2016, respectively. He joined the School of Communication and Information Engineering, Xi'an University of Posts and Telecommunications, China, in 2017. His research interests include green communications, cognitive radio, energy harvesting, and wireless-powered communications.

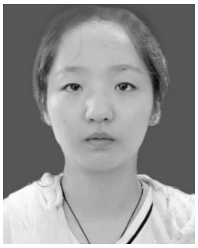

YINGYU BAI currently pursuing the bachelor's degree with the Xi'an University of Posts and Telecommunications. Her research interests include cognitive radio and spectrum sensing.

GUANGYUE LU received the Ph.D. degree from Xidian University, Xi'an, China, in 1999. From 2004 to 2006, he was a Guest Researcher with the Signal and Systems Group, Uppsala University, Uppsala, Sweden. Since 2005, he has been a Professor with the Department of Telecommunications Engineering, Xi'an Institute of Posts and Telecommunications, Xi'an. His current research interests include signal processing in communication systems, cognitive radio, and spectrum sensing.

JIN WANG received the Ph.D. degree from the University of Chinese Academy of Sciences, Beijing, China, in 2014. She was with the Chinese Academy of Sciences National Center from 2004 to 2016. She joined the School of Communication and Information Engineering, Xi'an University of Posts and Telecommunications, China, in 2017. Her research interests include 5G wireless networks, green communications, and cognitive radio.

HAIYAN HUANG received the B.Eng. degree in electronic and information engineering and the Ph.D. degree in military communication from Xidian University, Xi'an, China, in 2011 and 2016, respectively. She is currently a Lecturer with the School of Electronic and Information Engineering, Lanzhou Jiaotong University. Her research interests include cooperative transmission, non-orthogonal multiple access, and wireless sensor networks.